Journal of Materials Chemistry A

Accepted Manuscript

ROYAL SOCIETY OF CHEMISTRY

www.rsc.org/materialsA

Journal Name

ARTICLE

Enhanced charge transfer with Ag grids at electrolyte/electrode interfaces in solid oxide fuel cells

Mingi Choi, Sangyeon Hwang, Doyoung Byun* and Wonyoung Lee*

Received 00th January 20xx,
Accepted 00th January 20xx

DOI: 10.1039/x0xx00000x

www.rsc.org/

We systematically investigated the effect of Ag grids at the electrolyte/electrode interfaces on the electrochemical performance of solid oxide fuel cells (SOFCs). Electrohydrodynamic jet printing was employed to fabricate Ag grids with precise control of the geometry. A substantial reduction in the polarization resistance was observed when the pitch of the Ag grids decreased from 400 to 50 μm, indicating enhanced charge transfer through efficient supply and distribution of electrons along the Ag grids at the electrolyte/electrode interfaces. Our results demonstrate the possibility of engineering interfaces with metallic grids to achieve enhanced electrochemical performances for SOFCs operating at intermediate temperatures.

Introduction

Solid oxide fuel cells (SOFCs) have been promising as energy conversion devices because of their high potential in the development of thermal power plants with high conversion efficiency and environmental friendliness and without any environmentally harmful secondary products. However, the high operating temperatures (>800 °C) required for achieving reasonable ionic conductivity with conventional electrolyte materials are a significant limitation for practical applications.[1, 2] Therefore, extensive research using various approaches has been conducted to obtain intermediate operating temperatures (600-800 °C).[3-10]

At intermediate temperatures, oxygen reduction reaction (ORR) kinetics becomes extremely important because it has great influence on the electrochemical performance of the SOFC system.[11] Many perovskites have been investigated as candidate cathode materials because of their mixed ionic and electronic conductivity as well as their catalytic behavior towards the ORR. Among them, $La_{0.6}Sr_{0.4}Co_{0.2}Fe_{0.8}O_{3-\delta}$ (LSCF) has been considered a promising cathode material because of its relatively high ionic and electronic conductivity and fast oxygen exchange at intermediate temperatures.[12] Charge transfer reactions at the surface and interface, however, remain the rate-determining steps for LSCF at intermediate temperatures.[13] Recently, modified interface layers containing the metallic components with electrical conductivity and high catalytic activity have been systematically investigated to enhance charge transfer reactions using various methods, including composite cathodes, infiltration, electrodeless deposition, and sputtering.[4, 5, 14-18] Observed a significant improvement in charge transfer reactions and a ~16-fold increase in peak power density when they embedded a $Y_{0.08}Zr_{0.92}O_{2-\delta}$-Ag interlayer at electrolyte/electrode interfaces using DC and RF sputtering.[5] Zhou *et al.* achieved a ~1.7-fold performance increase by adding Ag in the bulk of $Ba_{0.5}Sr_{0.5}Co_{0.8}Fe_{0.2}O_{3-\delta}$ electrodes using the electrodeless deposition method.[18] However, those methods have no control over the geometry apart from the total amount of metallic components, resulting in blocking of effective reaction sites and a consequent decreasing in electrochemical performance.[4, 16, 18] Therefore, precise control of the geometry with the desired amount of metallic components is necessary to optimize the interfacial properties, and in turn, to maximize the electrochemical performance.

Electrohydrodynamic (EHD) jet printing method has been investigated for the high-resolution intuitive direct patterning of desired structures.[19, 20] An advantage of using electrical force to generate a jet of the target materials is that a fine pattern can be achieved on the micron-scale with control of the grid shape and pitch.[21] Moreover, EHD jet printing does not require vacuum, and has a short start-up time and fast printing velocity. Therefore, precisely controlled metallic grid structures can be fabricated at electrolyte/electrode interfaces using EHD jet printing, which has a high potential for application to large-scale SOFC systems.

In this study, we investigated the effects of Ag grids at electrolyte/electrode interfaces on electrochemical performance. EHD jet printing was employed to fabricate Ag grids at the electrolyte/electrode interface with precise control of the geometry. For systematic investigation, we printed Ag grids with various pitch values on the yttria-stabilized zirconia (YSZ) substrate in symmetric configuration. Electrochemical impedance spectroscopy (EIS) was used to assess the electrochemical performance. It was observed that the polarization resistance substantially decreased as the pitch of the Ag grid decreased. To

Department of Mechanical Engineering, Sungkyunkwan University

† Footnotes relating to the title and/or authors should appear here.
Electronic Supplementary Information (ESI) available: Zoom-in-view and 3-D profiler images along with the sheet resistance plots of fabricated the Ag grids with different pitches are given. See DOI: 10.1039/x0xx00000x

our best knowledge, this is the first report on the use of a printed metallic grid in the SOFC fabrication process for achieving enhanced electrochemical performance.

Experimental Details

EHD jet process

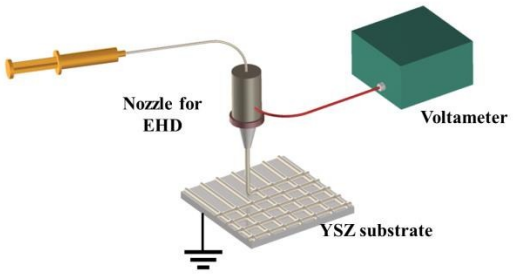

Fig. 1 Schematics of the EHD printing process.

A schematic representation of the EHD jet printing system is shown in Fig. 1. Printing was investigated with the commercial Ag ink used for EHD jet printing (ENJET), which is composed of Ag particles and a polymeric solution in the specific printing system (NP-200, ENJET). The printing system consisted of a ceramic nozzle with an inner diameter of 152 µm, a high voltage supplier, and a grounded collector whose position could be precisely controlled. For high-resolution printing, relative humidity and temperature were maintained at 45-47 % and 20-25 °C, respectively. Ag grids were printed symmetrically on both sides of a single crystal YSZ substrate (1 cm×1 cm, 8 mol%, MTI Korea), which is the most common material for SOFC electrolytes. The voltage difference between the nozzle and collector was 1.35 kV, while the nozzle-to-collector distance was maintained at 2.5 mm. The flow rate in the syringe pump (Harvard Apparatus) was maintained at 150 nL/min. The printing velocity was 150 mm/s. The pitch of the Ag grid was set as 50, 100, 200, and 400 µm.

Preparation of sample

After printing the Ag grids on the YSZ substrates, pre-sintering was performed at 200 °C for 2 h for removing the polymers and solvents. LSCF (Sigma-Aldrich Co.) powder was mixed with a binder (VEH, Fuel Cell Materials), and the resulting mixture was symmetrically printed on the sintered YSZ substrates at a thickness of ~20 µm. After screen printing, the samples were sintered at 800 °C for 4 h to evaporate the binders and to form the microstructure of the electrode. Electrodes were patterned with areas of 0.01, 0.04, 0.09, and 0.25 cm^2.

Characterization methods

Scanning electron microscopy (SEM, JSM7000F, JEOL) and 3D profiler (Nano View-100, Nanosystem Co.) were used to investigate the microstructure of the Ag grids and LSCF electrodes. A 4-point probe measurement system (MST-4000A, MS Tech.) was used to measure the in-plane sheet resistance of as-prepared samples with Ag grids having various pitch values. EIS measurements were performed using a custom-made test station in ambient air with an impedance analyzer (GAMRY Reference 600, GAMRY INC.) in the 0.01 Hz to 10^6 Hz frequency range.

Results and Discussion

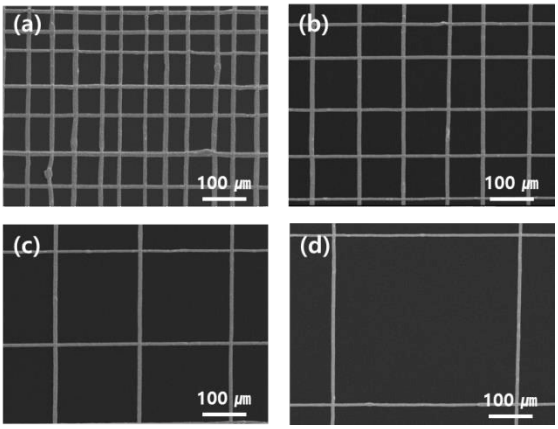

Fig. 2 SEM images of Ag grids. (a) 50 µm pitch (P50), (b) 100 µm pitch (P100), (c) 200 µm pitch (P200), and (d) 400 µm pitch (P400) .

To systematically investigate the effects of Ag grids at electrolyte/electrode interfaces on electrochemical performance, Ag grids with different pitches were fabricated. Fig. 2 shows SEM images of printed Ag grids after sintering at 200 °C for 2 h with pitch values of 50 µm (P50), 100 µm (P100), 200 µm (P200), and 400 µm (P400). Each grid has a width of 4-6 µm and a height of ~1.5 µm, as shown in Fig. S1 (see ESI). The Ag grid formed a continuous dense structure with a particle size of ~200 nm. Unexpectedly, some Ag particles were sputtered along the grids because the jet flow was sensitive to unwanted changes in the environment during printing. However, the influence of these particles on electrochemical performance can be considered negligible because of their small amount. In addition, cross-sectional images of the samples with and without Ag grids in Fig. S2 showed identical microstructures with a thickness of ~20 µm, confirming that deposition of the electrode layers was not affected by the Ag grids at the electrolyte/electrode interfaces. No significant structural instability, such as delamination of the electrode layer from the electrolyte, was observed.

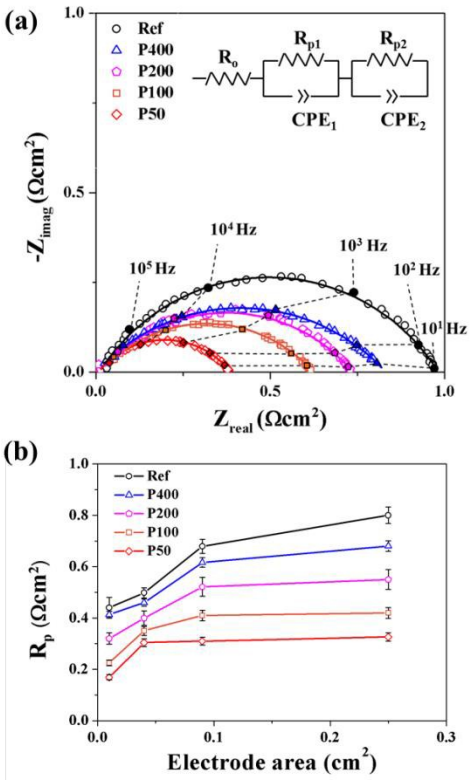

Fig. 3 EIS results of the symmetrical cells with different pitches at 650 °C: (a) Nyquist plot of samples with the equivalent circuit used for fitting. The electrode area was 0.01 cm^2 for all data. (b) Polarization resistance as a function of electrode area. Black, blue, pink, orange, and red markers represent the reference sample, P400, P200, P100, and P50, respectively.

To assess the effects of Ag grids on electrochemical performance, EIS measurements were performed in the 400-650 °C temperature range with a symmetric cell configuration. Fig. 3(a) shows the representative impedance spectra measured at 650 °C with a fitting curve using the equivalent circuit shown. The entire arc in the impedance spectra was assigned to the polarization resistance, R_p, *i.e.,* contributions from the electrode and electrolyte/electrode interface. The contribution from the electrolyte should be limited to the DC response because single crystal YSZ was used. A substantial reduction in R_p was observed when Ag grids were used. More interestingly, R_p decreased as the pitch of the Ag grids decreased. The R_p of the reference sample (with no Ag grids) with an area of 0.01 cm^2 was 0.44 Ωcm^2 at 650 °C. The R_p further decreased with Ag grids at the YSZ/LSCF interfaces to 0.41 Ωcm^2 in P400, 0.32 Ωcm^2 in P200, 0.22 Ωcm^2 in P100, and 0.17 Ωcm^2 in P50.

Fig. 3(b) shows R_p as a function of electrode area at 650 °C. The decrease in R_p with a decrease in pitch is clearly observed from all electrode areas tested in this study. Note that R_p increased as the electrode area increased. For example, the R_p of the reference sample increased from 0.44 to 0.79 Ωcm^2 as the electrode area increased from 0.01 to 0.25 cm^2. The observed increase in R_p with electrode area can be ascribed to the uneven charge distribution at the YSZ/LSCF interfaces, where the charge transfer reactions occur.[22-24] The R_p of samples with Ag grids also increased with electrode area, but with significantly suppressed amount. When the sample size increased from 0.01 cm^2 to 0.25 cm^2, R_p of the reference sample increased from 0.44 Ωcm^2 to 0.8 Ωcm^2, while R_p of P50 increased only from 0.17 Ωcm^2 to 0.32 Ωcm^2. More importantly, R_p of P50 in 0.25 cm^2 (the largest electrode area) is 26 % smaller than R_p of the reference sample in 0.01 cm^2 (the smallest electrode area). Our results demonstrate that the Ag grids at the electrolyte/electrode interfaces substantially improved the charge transfer reactions by providing electrons along the Ag grids evenly and effectively.

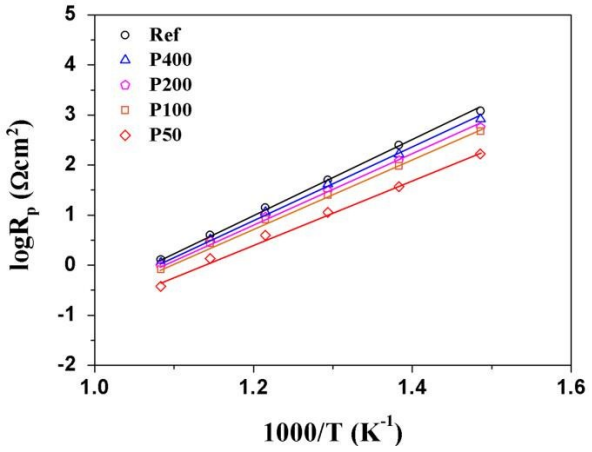

Fig. 4 Arrhenius plots of R_p vs. 1000/T. Black, blue, pink, orange, and red markers represent the reference sample, P400, P200, P100, and P50, respectively. The electrode area was 0.25 cm^2.

Fig. 4 shows the Arrhenius plot of R_p with more detail information about the origin of enhanced charge transfer reactions with the Ag grids. The slope in the Arrhenius plot represents the activation energy of oxygen reduction reaction (ORR). The activation energy of the reference sample, 1.48 eV, is well matched with reported value of 1.4-1.5 eV.[25-27] With Ag grids, the activation energy decreases: 1.41 eV for P400, 1.36 eV for P200, 1.34 eV for P100, and 1.27 eV for P50. This decrease in activation energy suggests changes in the rate-limiting step of the ORR in the presence of Ag grids. Recently, Muranaka *et al.* also reported a smaller activation energy with the LSCF-Ag cermet cathode (~1.3 eV) compared to the pure LSCF cathode (~1.5 eV).[26] Xiong *et al.* reported activation energies of ~1.1 eV for surface reactions and ~1.34 eV for interfacial reactions at dense LSCF thin-film cathodes.[28] Therefore, we conclude that the rate-limiting step of the LSCF electrodes changed from interfacial reactions to the oxygen surface exchange reactions with Ag grids at the electrolyte/electrode interfaces. This decrease in activation energy with the smaller pitch further confirms that Ag grids at the electrolyte/electrode interfaces can improve the charge transfer reactions between the electrolyte and electrode.

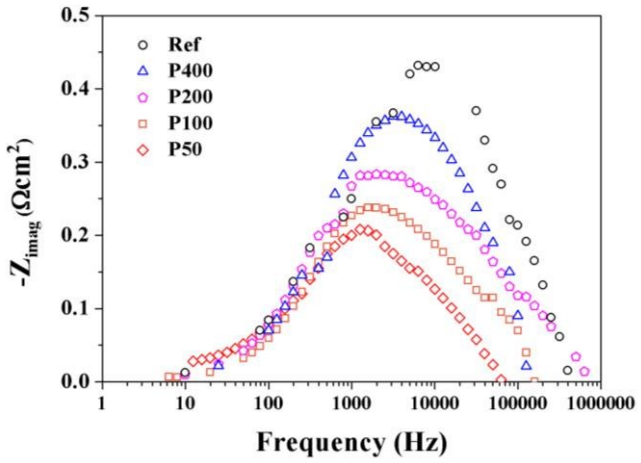

Fig. 5 Bode plots at 650 °C with an electrode area of 0.25 cm^2. Black, blue, pink, orange, and red markers represent the reference sample, P400, P200, P100, and P50, respectively.

Fig. 5 shows the Bode plot of EIS spectra measured at 650 °C. The reference sample showed a peak frequency of approximately ~10^4 Hz. The specific frequency at which the peak is located represents the rate-limiting step in the electrochemical reactions.[13, 18, 29-35] The rate-limiting step in the frequency range of 10^4-10^5 Hz is attributed to the charge transfer reactions at the electrolyte/electrode interfaces.[18, 29, 30, 32, 35] As the pitch of the Ag grids became smaller, the imaginary components in this frequency range were suppressed, indicating significant improvement in the charge transfer reactions in the presence of the Ag grids. This is in concurrence with a similar observation that the metallic cermet improves charge transfer reactions because of its high electrical conductivity.[4, 15, 26, 36] Charge transfer reactions of SOFCs require electrons when dissociated oxygen ions are reduced and incorporated into the oxygen vacancies in the electrolyte. Fast delivery of electrons along the Ag grids at the electrolyte/electrode interfaces may improve the kinetics of oxygen reduction, which the most sluggish reaction step. Further suppression, with a smaller pitch, substantiates that the number of active reaction sites at which charge transfer reactions occur increased in the presence of Ag grids. In addition, the peak frequency was shifted to a lower value, e.g. ~10^3 Hz for P50, indicating that the rate-limiting step changed substantially. The rate-limiting step in the frequency range of 10^2-10^4 Hz is attributed to oxygen exchange reactions at the electrode surfaces. The results from the frequency analysis were consistent with the activation energy analysis, where the Ag grids at the electrolyte/electrode improved charge transfer reactions between the electrolyte and electrode through the efficient supply and distribution of electrons along the Ag grids.

However, it is worth noting that the Ag grids may have an adverse effect on the electrochemical performance beyond a certain limit. Guo *et al.* reported that the ORR kinetics could be disturbed by excess Ag because of blocking of the active reaction sites at the surface and interfaces. Lee *et al.* also reported that the performance increased with the addition of 3 wt% of Ag, but decreased with the addition of 5 wt% of Ag.[15, 16] Even though the electrochemical performance increased with a smaller pitch in this study, there should be balance between the advantages and disadvantages of the Ag grids. As Ag covers more of the YSZ surface with smaller pitch values, the number of reaction sites at the electrolyte/electrode interfaces decreases, reducing the performance. In addition, given the high mobility of Ag may impose the stability issue at elevated temperatures. Exploring the optimal geometry of the Ag grids for maximized performance and stability will be a subject of future work.

Conclusions

We investigated the effects of Ag grids at the electrolyte/electrode interfaces on enhancing the charge transfer reactions of SOFCs. The Ag grids substantially enhanced the charge transfer reactions at electrolyte/electrode interfaces. Higher enhancement was observed with smaller pitch values of the Ag grids, confirming that the efficient supply and distribution of electrons at the electrolyte/electrode interfaces can facilitate ORR kinetics. Our results clearly demonstrate the significant potential of EHD jet printing as a fabrication method for systematic investigation of the relationship between grid structures and electrochemical performances, and for studying large-scale SOFC systems not limited to lab-scale experiments.

Acknowledgements

This research was supported by the Basic Science Research Program through the National Research Foundation of Korea (NRF) funded by the Ministry of Science, ICT & Future Planning (Grant No. NRF-2013R1A1A1059845).

References

1 E. D. Wachsman and K. T. Lee, *Science,* **2011**, 334, 935-939.
2 K. T. Lee, A. A. Lidie, S. Y. Jeon, G. T. Hitz, S. J. Song and E. D. Wachsman, *J. Mater. Chem. A*, **2013**, 1, 6199.
3.W. Lee, H. J. Jung, M. H. Lee, Y.-B. Kim, J. S. Park, R. Sinclair and F. B. Prinz, *Adv. Funct. Mater.*, **2012**, 22, 965-971.
4 L.-P. Sun, H. Zhao, Q. Li, L.-H. Huo, J.-P. Viricelle and C. Pijolat, *Int. J. Hydrog. Energy*, **2013**, 38, 14060-14066.
5 S. H. Choi, C. S. Hwang and M. H. Lee, *ECS Electrochem. Lett.*, **2014**, 3, F57-F59.
6 Y. K. Li, H. J. Choi, H. K. Kim, N. K. Chean, M. Kim, J. Koo, H. J. Jeong, D. Y. Jang and J. H. Shim, *J. Power Sources*, **2015**, 295, 175-181.
7 J. S. Park, J. An, M. H. Lee, F. B. Prinz and W. Lee, *J. Power Sources*, **2015**, 295, 74-78.
8 J. H. Shim, S. Kang, S.-W. Cha, W. Lee, Y. B. Kim, J. S. Park, T. M. Gür, F. B. Prinz, C.-C. Chao and J. An, *J. Mater. Chem. A*, **2013**, 1, 12695.
9 J. An, J. H. Shim, Y. -B. Kim, J. S. Park, W. Lee, T. M. Gür and F. B. Prinz, *MRS Bull.*, **2014**, 39, 798-804.
10 J. Park, I. Chang, J. Y. Paek, S. Ji, W. Lee, S. W. Cha and J. -M. Lee, *CIRP Ann-Manuf. Technol.*, **2014**, 63, 513-516.
11 Z. Sun, E. Fabbri, L. Bi and E. Traversa, *Phys. Chem. Chem. Phys*, **2011**, 13, 7692-7700.
12 M. Katuski, S. Wang, M. Dokiya and T. Hashimoto, *Solid state ion.,* **2003**, 156, 453-461.
13 S. B. Adler, *Chem. Rev.,* **2004**, 104, 4791-4843.
14 V. A. C. Haanappel, D. Rutenbeck, A. Mai, S. Uhlenbruck, D. Sebold, H. Wesemeyer, B. Röwekamp, C. Tropartz and F. Tietz, *J. Power Sources*, **2004**, 130, 119-128.
15 K. T. Lee and A. Manthiram, *J. Power Sources*, **2006**, 160, 903-908.

16 S. Guo, H. Wu, F. Puleo and L. Liotta, *Catalysts*, **2015**, 5, 36-391.
17 S. Wang, T. kato, S. Nagata, T. Kaneko, N. Iwashita, T. Honda and M. Dokiya, *Solid state ion.,* **2002**, 152-153, 477-484.
18 W. Zhou, R. Ran, Z. Shao, R. Cai, W. Jin, N. Xu and J. Ahn, *Electrochim. Acta*, **2008**, 53, 4370-4380.
19 J. U. Park, M. Hardy, S. J. Kang, K. Barton, K. Adair, D. K. Mukhopadhyay, C. Y. Lee, M. S. Strano, A. G. Alleyne, J. G. Georgiadis, P. M. Ferreira and J. A. Rogers, *Nat. Mater*, **2007**, 6, 782-789.
20 Y. Huang, N. Bu, Y. Duan, Y. Pan, H. Liu, Z. Yin and Y. Xiong, *Nanoscale*, **2013**, 5, 12007-12017.
21 Y. Jang, J. Kim and D. Byun, *J. Physics D-Appl. Phys.*, **2013**, 46, 155103.
22 F. P. F. van Berkel, F. H. van Heuvelen and J. P. P. Huijsmans, *Solid state ion.,* **1994**, 72, 240-247.
23 J. Fleig and J. Maier, *J. Electrochem. Soc.,* **1997**, 144, L302-L305.
24 T. Kenjo and Y. Kanehira, *Solid state ion.,* **2002**, 148, 1-14.
25 D. Waller, J. A. Lane, J. A. Kilner and B. C. H. Steele, *Solid state ion.,* **1996**, 86-88, 767-772.
26 M. Muranaka, K. Sasaki, A. Suzuki and T. Terai, *J. Electrochem. Soc.*, **2009**, 156, B743.
27 V. Dusastre and J. A. Kilner, *Solid state ion.,* **1999**, 126, 163-174.
28 H. Xiong, B.-K. Lai, A. C. Johnson and S. Ramanathan, *J. Power Sources*, **2009**, 193, 589-592.
29 H. N. Im, M. B. Choi, S. Y. Jeon, S. Bhupendra and S. J. Song, *ECS Trans.,* **2014**, 61, 347-352.
30 I. M. Torres da silva, J. Nielsen, J. Hielm and M. Mogensen, *ECS Trans.,* **2009**, 25, 489-498.
31 J. R. Smith, A. Chen, D. Gostovic, D. Hickey, D. Kundinger, K. L. Duncan, R. T. DeHoff, K. S. Jones and E. D. Wachsman, *Solid State Ionics*, **2009**, 180, 90-98.
32 M. J. Jørgensen and M. Mogensen, *J. Electrochem. Soc.*, **2001**, 148, A433.
33 R. Barfod, M. Mogensen, T. Klemensø, A. Hagen, Y.-L. Liu and P. Vang Hendriksen, *J. Electrochem. Soc.*, **2007**, 154, B371.
34 Y. L. Yang, C. L. Chen, S. Y. Chen, C. W. Chu and A. J. Jacobson, *J. Electrochem. Soc.,* **2000**, 147, 4001-4007.
35 Z. Jiang, Z. Lei, B. Ding, C. Xia, F. Zhao and F. Chen, *Int. J. Hydrog. Energy*, **2010**, 35, 8322-8330.
36 Q. Li, L.-P. Sun, L.-H. Huo, H. Zhao and J.-C. Grenier, *J. PowerSources,* **2011**, 196, 1712-1716.